Non-Equilibrium Phase Separation and Dynamics of Active Systems in Harmonic Trap Potential

Avinash Gupta

A dissertation submitted for the partial fulfilment
of BS-MS dual degree in Science

Indian Institute of Science Education and Research Mohali
April 2018

Certificate of Examination

This is to certify that the dissertation titled **Non-Equilibrium Phase Separation and Dynamics of Active Systems in Harmonic Trap Potential** submitted by **Avinash Gupta** (Reg. No. MS13114) for the partial fulfillment of BS-MS dual degree programme of the Institute, has been examined by the thesis committee duly appointed by the Institute. The committee finds the work done by the candidate satisfactory and recommends that the report be accepted.

Dr. Samir Kumar Biswas   Dr. Rajeev Kapri   Dr. Abhishek Chaudhuri (Supervisor)

Dated: April 20, 2018

Declaration

The work presented in this dissertation has been carried out by me under the guidance of Dr. Abhishek Chaudhuri at the Indian Institute of Science Education and Research Mohali.

This work has not been submitted in part or in full for a degree, a diploma, or a fellowship to any other university or institute. Whenever contributions of others are involved, every effort is made to indicate this clearly, with due acknowledgement of collaborative research and discussions. This thesis is a bonafide record of original work done by me and all sources listed within have been detailed in the bibliography.

Avinash Gupta

(Candidate)

Dated: April 20, 2018

In my capacity as the supervisor of the candidate's project work, I certify that the above statements by the candidate are true to the best of my knowledge.

Dr. Abhishek Chaudhuri

(Supervisor)

Acknowledgment

It has been a very pleasant experience working with my Supervisor: Dr. Abhishek Chaudhuri. He has been very helpful and encouraging at every stage of this project. I feel lucky to get the opportunity to work with him. He was very patient, flexible and guiding in making this work a progress. I would like to thank Dr. Rajeev Kapri who helped me in coding whenever I required help and i would also like to thank my committee member, Dr. Samir k. Biswas for variable comments and suggestions.

I am also very thankful to my colleagues for encouraging me throughout the project. Lastly, I would like to thank my family for the moral support and strength.

List of Figures

Abstract

We have used theoretical models to study individual motion of active particle as well as collective dynamics and pattern formation in active particles. There are many examples of active units that you can see in biological and complex physico-chemical systems are motile cells, patterns which is localized in reaction-diffusion system, chemically powered nano-rods or macroscopic animals. So here i am using the stochastic differential equations to study the individual and collective motion of point-like active particles in harmonic trap potentials. We characterized the active system by using radial distribution and virial pressure.

We performed parallel-molecular dynamic simulations on a model for active systems for diferent Peclet numbers and for several system sizes. We have shown from numerical studies that this active colloidal system phase separates. Then we have also studied the dynamics of a brownian circle swimmer in a trap potential which is harmonic. I have also shown the results in different conditions like time-varying self-propulsion and harmonic tap potential and found the periodic trajectories which is stable in the absence of brownian noise and if we include noise then the trajectories become spiral and collapse into trap center.

Contents

Chapter 1

Introduction

How do we distinguish between "dead" matters and "living ones"? What variables do we choose to describe systems thst are living, i.e. those use energy from the environment to propel themselves. These are imprtant questions to answer in order to study living matter.

In this thesis, we look at active systems in confinement and otherwise. We study individual and collective dynamics of the active particles.

1.1   Active Matter

Active motion might be defined as a motion of particles or agents under the influence of an internal driving force. This driving force can have different origin such as non-equilibrium dynamics in an artificial driven system or activities that are biological in nature. It is basically different from the behaviour of dynamic of purely passive particles in solids, liquids and gaseous states at thermal equilibrium. Active particles have an internal propulsion mechanism, which use the energy from external environment and then convert into directed motion.

The most common example of an active matter system is the flock of birds. Each birds use its own energy to fly. Even though each of the bird is moving in its independent trajectory, but the collection of birds as whole form coherent pattern.

We cannot neglect fluctuations in these systems. Fluctuations can be internal or from external environment. Therefore, our model system should include the effect of noise.

Vicsek model was first introduced in 1995 and proved to be an important theoretical study. In the experimental side, studies were done on bacteria, school of fish and starlings. As discussed earlier, since energy is constantly pumped into the system,
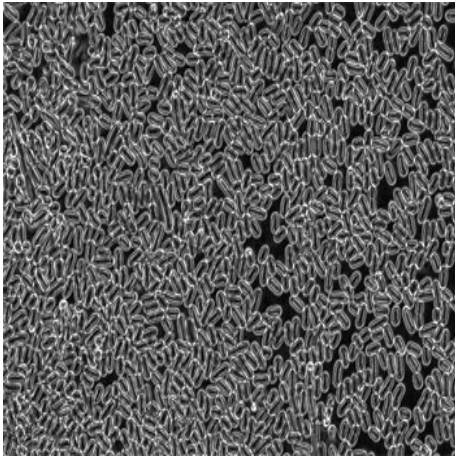
[1]   [2]

(a)   (b)

[3]

(c)

Figure 1.1: Examples of active matter systems. (a)School of fish , (b)Flock of starlings, (c)Bacterial suspension .

particles maintain a certain velocity. Vicsek model showed that self organized state can emerge from a disordered state by taking activity. Active systems fall into the class of non-equilibrium system where one cannot apply the thermodynamical concepts like the Helmholtz free energy. The propulsive motion of particles can even lead to phase separation in monodisperse systems of pure repulsive particles.

1.2   Brownian Motion

The motion of particles suspended in a fluid like gas or water is often described by Brownian motion.

Time evolution of a free brownian particle is given by the Langevin equation,

$$m\dot{v} = -m\gamma v + \eta(t) \tag{1.1}$$

where m and v represent mass and instantaneous velocity of the Brownian particle. In this equation you can see two force parts because of effect of liquid medium on the motion of brownian particle:

1. First part is $m\gamma = \zeta$, which shows that there is a dynamical friction which experienced by the particle.

2. Second part is fluctuating force, coming due to the kicks from solvent particles.

In Brownian motion, particles continuously collide with molecules present in the fluid. The frequency of such collision is of the order of 10^{21} per second. Hence it is not possible to use deterministic equation for these particles doing Brownian motion. If the positions and velocities of all the molecules in the fluid are known at a given point of time then one can in principle calculate the force uniquely. However, practically it is impossible to keep track of all the particles. Hence a stochastic approach is needed to address this problem. Assume that there exist arbitrary time interval $dt = t - t'$ such that $\eta(t)$ and $\eta(t')$ are uncorrelated and v is free to change.

$$\langle \eta(t) \rangle = 0 \tag{1.2}$$

$$\langle \eta(t)\eta(t') \rangle = \Gamma \delta(t - t') \tag{1.3}$$

where Γ determines strength of these fluctuations. Equation (1.2) implies that there is no preferred direction for the random force.

Mean square displacement of a particle satisfying the Langevin equation is given by,

$$\langle X(t)^2 \rangle = \frac{2k_B T}{m\gamma^2}[\gamma t - 1 + exp(-\gamma t)] \tag{1.4}$$

At very long times, as $t \to \infty$, particle is in the diffusion regime and

$$\langle X(t)^2 \rangle = \frac{2k_B T}{m\gamma}t = 2Dt \tag{1.5}$$

At short time limit ($t \longrightarrow 0$), From eq.1.4

$$\langle X(t)^2 \rangle = \frac{2k_BT}{m}t^2 \tag{1.6}$$

In the short time, the mean square displacement is proportional to t^2 and you can see that it is independent of the nature of the liquid.

From the Langevin equation, velocity auto-correlation function can be obtained,

$$\langle v(t)^2 \rangle = v(0)^2 e^{-2\gamma t} + \frac{\Gamma}{2m^2\gamma}[1 - e^{-2\gamma t}] \tag{1.7}$$

At long times system reaches equilibrium and mean square velocity is given by the Boltzmann distribution,

$$\langle v(t)^2 \rangle = \frac{k_BT}{m} \tag{1.8}$$

From eqn. (1.7) and eqn. (1.8),

$$\Gamma = 2m\gamma k_BT \tag{1.9}$$

It is the fluctuation-dissipation relation. It relates magnitude of fluctuations (Γ) to the strength of frictional force (γ) which causes dissipation.

Plan of Thesis

In this project we present simulation and theory based studies of an active system using a minimal model of self-propelled Brownian disks interacting only via the excluded-volume repulsive potential. The phase separation of self-propelled disks in two dimensions was investigated. Then we considered a single active particle in a harmonic trap and characterized its dynamics. Finally we looked at the collective dynamics of active particles in harmonic trap.

Chapter 2

Phase Separation in Active System

In this chapter, we study the collective dynamics of self propelled particles in a minimal model. The particle interact via a repulsive potential. Here, one would not expect clustering in a passive system of such particles. However, activity in the term of self propulsion leads to clustering and a phase seperation.

2.1   Model and Simulation Methods

In the model, particles are characterized by their position r_i and orientation θ_i. The particles move with a constant velocity along their orientations. The orientation undergo free rotational diffusion. Therefore the overdamped dynamics of position and orientation are given by,

$$\dot{r}_i = D\beta[F_{ex}(r_i) + F_p\hat{\mathbf{v}}_i] + \sqrt{2D}\eta_i^T \tag{2.1}$$

$$\dot{\theta}_i = \sqrt{2D_r}\eta_i^R \tag{2.2}$$

where, $F_{ex}(r) = -\frac{dU_{ex}(r)}{dr}$.
$U_{ex}(r)$ is called the WCA potential, given by,

$$U_{ex}(r) = \begin{cases} 4\epsilon\left[\left(\frac{\sigma}{r}\right)^{12} - \left(\frac{\sigma}{r}\right)^6 \right] + \epsilon & \text{if } r < 2^{\frac{1}{6}} \\ 0 & \text{otherwise} \end{cases} \tag{2.3}$$

σ is particle diameter, $\epsilon = k_B T$. This is a short range repulsive potential. D_r and D are rotational and translational diffusion coefficients. In the low Reynolds number(a dimensionless parameter that compares the effect of inertial and viscous forces) regime,

i.e. in the overdamped regime, they are related as

$$D_r = \frac{3D}{\sigma^2} \tag{2.4}$$

F_p is the magnitude of active force which gives rise to a velocity(in the absence of interaction).

$$\mathbf{v}_p = D\beta F_p \hat{\mathbf{v}}_i \tag{2.5}$$

where,

$$\hat{\mathbf{v}}_i = \begin{pmatrix} \cos\theta_i \\ \sin\theta_i \end{pmatrix} \quad , \quad \beta = \frac{1}{k_B T} \tag{2.6}$$

η are the uncorrelated Gaussian noise,

$$\langle \eta_i(t) \rangle = 0 \quad \text{and} \quad \langle \eta_i(t)\eta_j(t') \rangle = 2D\delta_{ij}\delta(t - t') \tag{2.7}$$

Equations of motion are non-dimensionalized using σ, $k_B T$ and $\tau = \frac{\sigma^2}{D}$ as basic units of length, energy and time respectively. The system is parametrised by two functions, system density ρ ($\rho = \frac{N^2}{L^2}$), where N is total number of particles in the system and L is system length) and the Péclet number Pe [1]. Péclet number is same as the non-dimensionalized self-propulsion velocity,

$$Pe = \frac{v_p \tau}{\sigma} \tag{2.8}$$

We employed molecular dynamics simulation technique to integrate the equations of motion. Integration of stochastic equations (4.1 and 4.2) were established using the stochastic Euler scheme. Time constraint was one of the major difficulty we have encountered during execution. For a system of N particles, calculation of resultant potential on a single particle requires time-steps of the order of N^2. Parallel programming techniques using OpenMP were used to reduce simulation time for calculating pair-wise interactions. We have successfully been able to reduce this exponential time requirement by threading the loops.

---

[1]Péclet number is defined as ratio of bulk flow of a quantity to rate of diffusion of the same quantity,

$$Pe = \frac{\text{rate of advection}}{\text{rate of diffusion}}$$

2.2 Simulation Results

2.2.1 Phase Separation

Here, we have performed simulation with $N = 5000$ particles at a fixed density of $\rho = 0.7$. The results for $Pe = 10$, 50 and 90 are shown in fig. 2.1. As we can see, for $Pe = 10$, the system is homogeneous in the steady state. The local density distribution is peaked about the system density. When we start increasing the Pe, then at $Pe = 50$, we start observing clusters. The local density distribution is now broad indicating the presence of these clusters. At very high $Pe = 100$, we observe a phase separation, with the emergence of large clusters. Now, the local density distribution shows two peaks - a dense phase of density higher than the system density and a dilute phase with density less than the system density.

The phase separation is similar to what is observed in passive systems with particles undergoing attractive interactions. However in this system, there is neither attractive interaction nor an alignment mechanism. The self propulsion coupled with the excluded volume interaction gives rise to a self trapping mechanism - particles get stuck and block each other. This leads to the phase separation into dense and dilute phases.
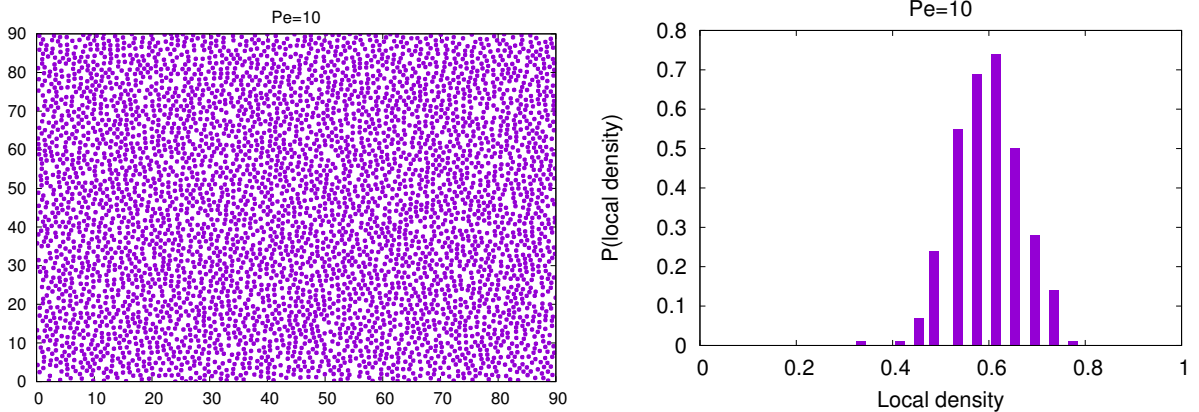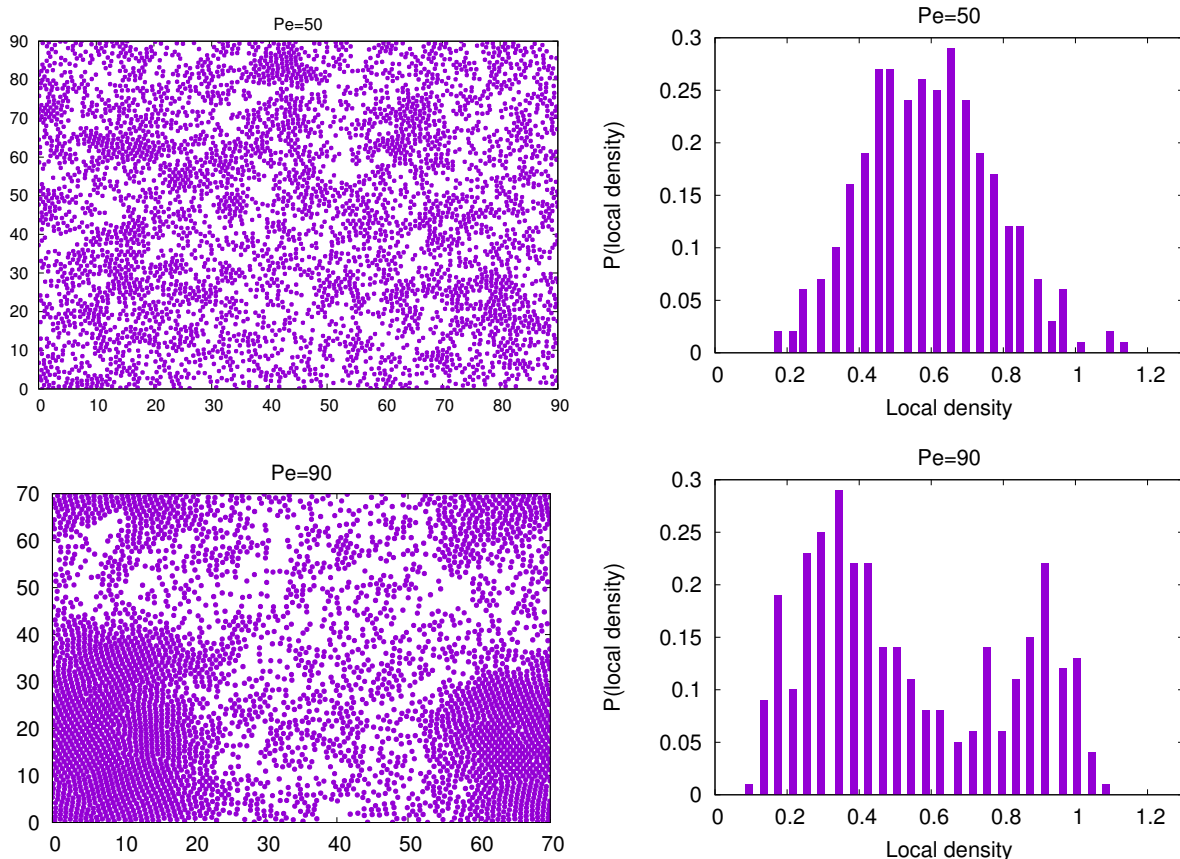
Figure 2.1: (left) snapshot of the system configuration for different Pe (right) corresponding local density distributions. Distribution corresponding to the single density flattens and broadens as Pe is increased and make binodal as the system phase separates. N = 5000, Average density = 0.7, Time-steps = 20 x $10^5 dt$.

2.2.2   Pair Correlation

The radial distribution function or the pair correlation function g(r), is the probability of finding a particle at a distance r from a reference particle, relative to the probability for an ideal gas. This gives the density variation as a function of the distance from reference particle.

In this active system, we observe that at a given value of the interaction strength ϵ, the position of first peak of g(r) shifts towards smaller r with increasing Pe. In the fig. 2.2, we compare g(r) for Pe=0 and Pe=30. At Pe=30, the peaks shifts to the left. Higher Pe means higher speeds of the self propelled particles. The particles can enter further into the repulsive regime of the interaction potential between particles. Therefore it becomes more probable to observe particles at close distances, giving rise

to higher peaks.

If the interaction strength is varied, keeping the Pe constant, then the effect is not as much. The pair correlation function for $\epsilon = 4$ and $\epsilon = 1$ are shown in the fig. 2.3. The peak shift slightly towards larger separation with increasing ϵ. However, there is very small changes in the peak heights.

So, here we see how activity of active fluid system affect the pair correlation of system. So we can see in the fig2.2, with increasing peclet(Pe=0 to 30) the size of the first peak of pair distribution function increase in height and shifts towards smaller distances.

In the case of higher peclet number, probability of observing smaller particle separations increases, since particles are able to more easily enter the repulsive domain of the interaction force. In the case of larger separations, pair correlation function g(r) falls below the active one. As a consequence, particle separations are moved to smaller values.
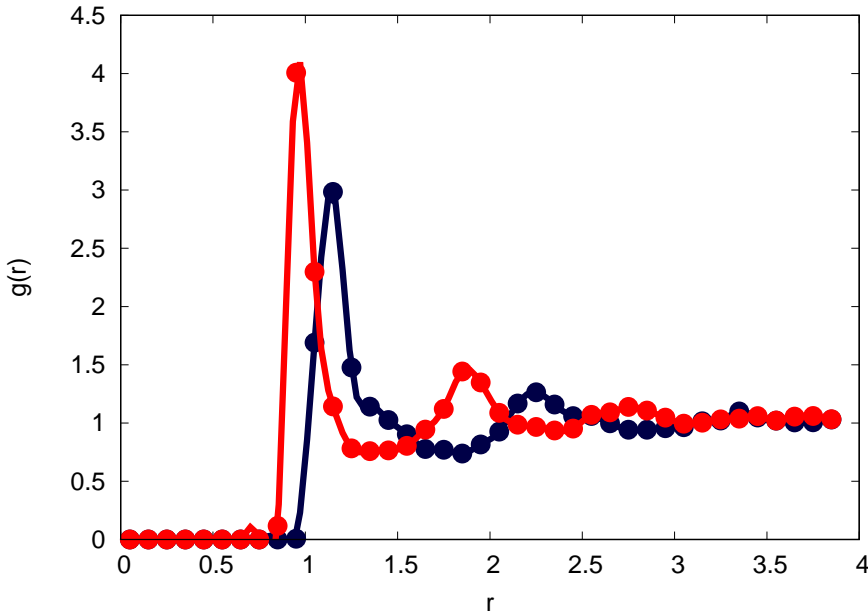

Figure 2.2: Comparision of pair distribution function with increasing Pe , red(Pe=30) and blue(Pe=0).

So increasing interaction parameter ϵ which controls strength of repulsion between particles, for the WCA potential at fixed peclet number(Pe= 30), so we can see in the fig 2.3, the first peak of the pair distribution function increases in height while its position moves to larger particle separations.
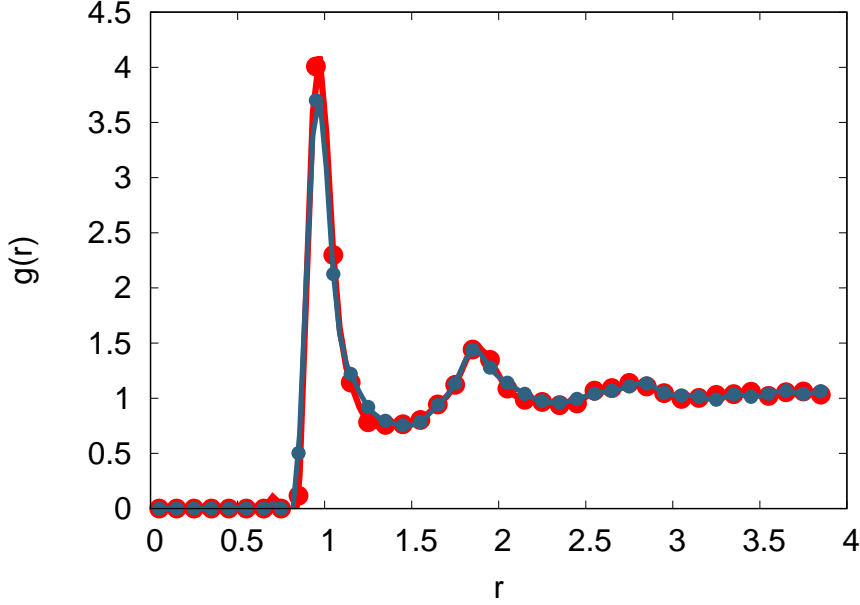
Figure 2.3: Comparision of pair distribution function with increasing ϵ, red($\epsilon = 4$) and grey($\epsilon = 1$).

2.2.3 Virial Pressure

Virial pressure for a two dimensional active system is given as,

$$P = \frac{\rho}{2N}[v_p \Sigma_i \langle \hat{v}_i . r_i \rangle + 48 \Sigma_{i<j} \langle r_{ij} . F_{ij} \rangle] \tag{2.9}$$

where $\langle \cdot \rangle$ is the steady state average. The second term in the expression is the usual expression for virial pressure for system of passive interacting particles. The first term gives the active contribution.

We see in fig. 2.4, that the virial pressure for active system increases with increasing activity at a fixed value of interaction strength. At a fixed Pe, the virial pressure increase with increasing strength of interaction. Increasing ϵ, implies stronger repulsion leading to increasing virial pressure.
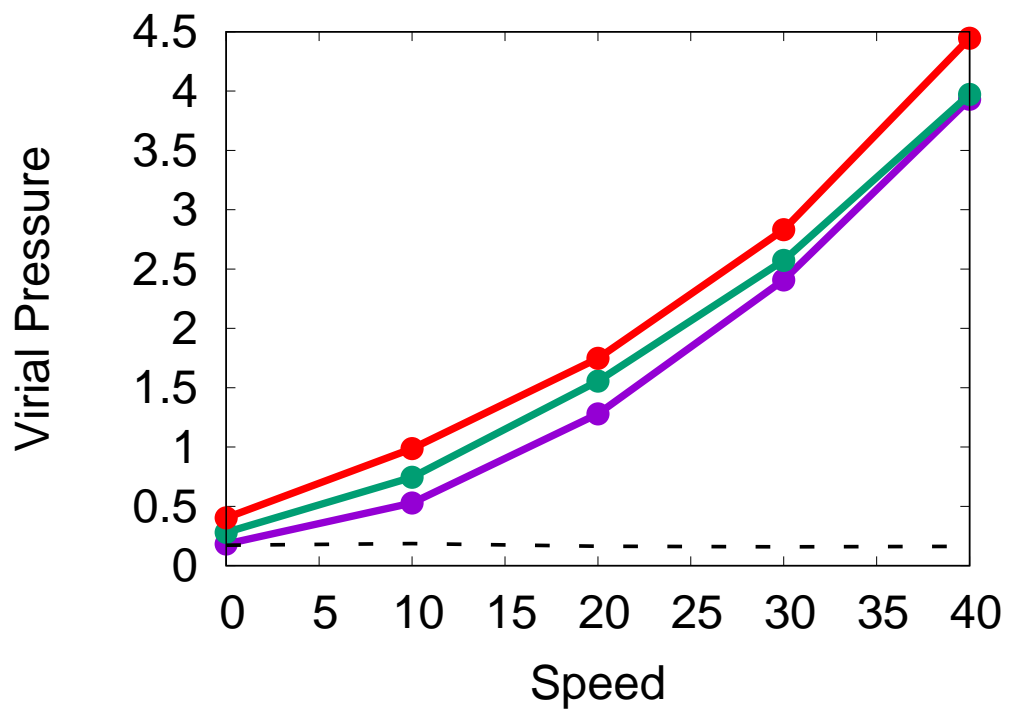
Figure 2.4: Comparision of virial pressure for different potential strengths ϵ, red($\epsilon = 4$), green($\epsilon = 2$), purple($\epsilon = 0.5$) and dotted line($\epsilon = 4$, $Pe = 0$).

Chapter 3

Brownian Motion of a Circle Swimmer in a Harmonic Trap

Studying the dynamics of particles trapped by potentials, is important in many scenarios, such as colloids in optical tweezers and motion of tracers in a matrix. In this study, we try to look at the dynamics of a single active particle in a trap under different trap conditions. This based on the study of Soudeh Jahanshahi et al.[8]

Model and Simulation

Here we are using the overdamped langevin equations to study the brownian motion of single particle in a 2D harmonic trap. Here we are taking harmonic potential symmetric which is centered at the origin. [8]

$$V(r) = \frac{\gamma}{2}r^2 \tag{3.1}$$

where $r^2 = x^2 + y^2$ and γ is trap strength of harmonic potential .

3.1 Constant F_p and Constant $F_{harmonic}$

In the overdamped limit condition, the translation motion of single particle in 2D plane is given as

$$\dot{r}(t) = D\beta\left[F_p\hat{\mathbf{v}}(t) - \gamma r(t)\right] + \sqrt{2D}\eta^T(t) \tag{3.2}$$

Unlike the previous study, we here are looking at a circle swimmer, which undergoes active rotational motion with self propulsion. Therefore, for the angle $\theta(t)$

rotational motion is given by langevin equation

$$\dot{\theta}(t) = \sqrt{2D_r}\eta^R(t) + w \tag{3.3}$$

where, w models an effective torque and results in chiral motion. D_r and D are rotational and translational diffusion coefficients.

(a) Results in the case of zero noise

Here i am considering the situation in the case of zero thermal noise, i.e., $\eta^T(t) = \eta^R(t) = 0$ and in this condition, equation of motion are given as ,

$$\frac{x(t)}{R} = e^{-\gamma D_r t}[c_x + f(D_r t, w, \theta_0, \gamma)] \tag{3.4}$$

and

$$\frac{y(t)}{R} = e^{-\gamma D_r t}[c_y + f(D_r t, w, \theta_0 - \frac{\pi}{2}, \gamma)] \tag{3.5}$$

where $c_x = x_0/R$ and $c_y = y_0/R$ and (x_0, y_0) is initial position of center of mass of particle and here f is function which is given by

$$f(t, w, \theta, \gamma) = \frac{F_p}{\gamma^2 + w^2}[\gamma e^{\gamma t}cos(wt + \theta) + we^{\gamma t}sin(wt + \theta) - \gamma cos(\theta) - wsin(\theta)] \tag{3.6}$$
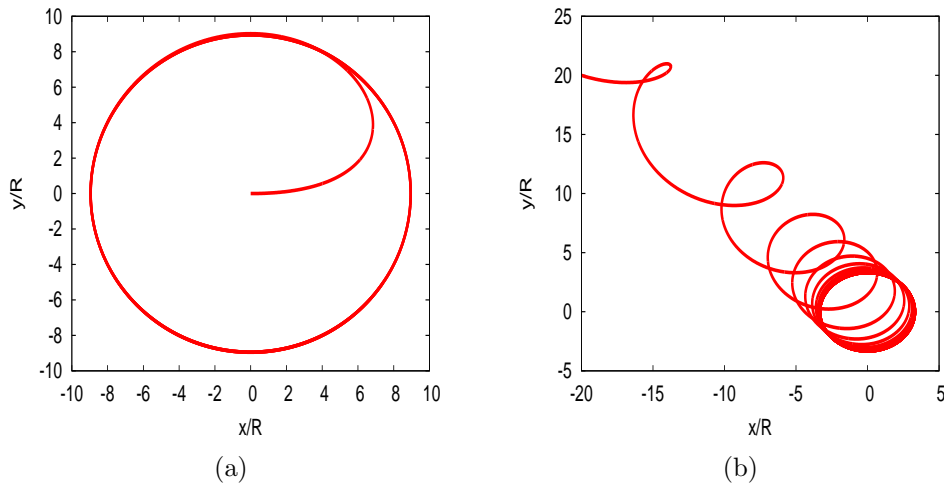

Figure 3.1: Nose free trajectories with constant F_p in constant harmonic trap, $F_p = 100$ and $\theta_0 = 0$:(a)$\gamma = 10$, $c_x = c_y = 0$ and $w = 5$, (b)$\gamma = 3$, $c_x = -20$, $c_y = 20$ and $w = 30$.

14

Corresponding to these equations, we get the trajectories results in different conditions fig3.1. For small ratio w/γ particle approaches final trajectories in form of circular but for higher ratio it take some revolutions until regular periodic motion is achieved.

(b) In the presence of Brownian noise

In the presence of thermal noise, the motion of equations are obtained by averaging over noise terms

$$\frac{\langle x(t)\rangle}{R} = e^{-\gamma D_r t}[c_x + f(D_r t, w, \theta_0, \gamma - 1)] \tag{3.7}$$

and

$$\frac{\langle y(t)\rangle}{R} = e^{-\gamma D_r t}[c_y + f(D_r t, w, \theta_0 - \frac{\pi}{2}, \gamma - 1)] \tag{3.8}$$

So you can see in fig 3.2, the noise averaged trajectories make spiral curves which collapse into trap center and reason for this behavior is because of the factor $e^{-D_r t}$ which comes from rotational brownian motion. Although a deterministic torque causes uniform rotation around the center of trap, the random noise leads to the reduction of the radius, finally collapsing at he center of the trap.
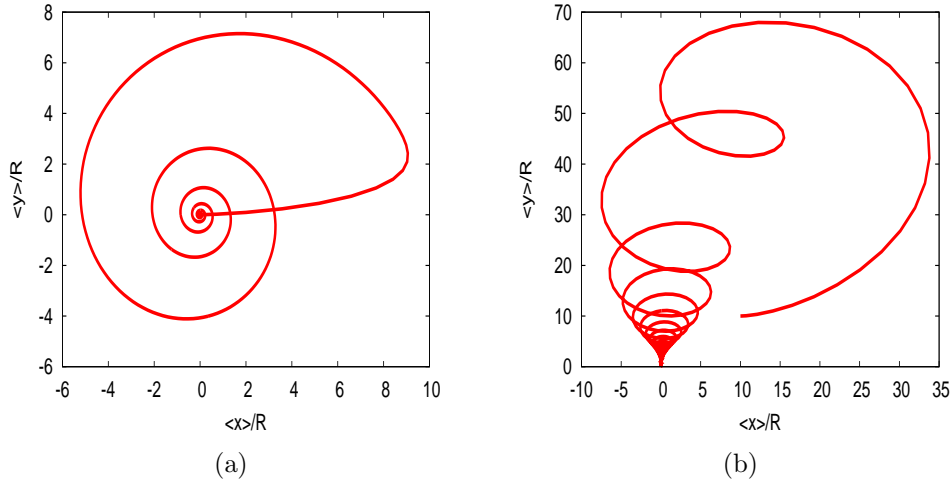

(a) (b)

Figure 3.2: Nose averaged trajectories with constant self propulsion in constant harmonic trap $F_p = 100$ and $\theta_0 = 0$:(a)$\gamma = 10$, $c_x = c_y = 0$ and $w = 7$, (b)$\gamma = 0.7$, $c_x = c_y = 0$ and $w = 10$.

3.2 Time-Dependent Self-Propulsion

Here we take self-propulsion time dependent and study the dynamics of a circle swimmer in harmonic trap. The equation for self-propulsion form is,

$$F_p(t) = F_{p_0}[1 + cos(\nu t + \phi)]\hat{u}. \tag{3.9}$$

where ν is propulsion frequency and ϕ is the initial phase.

Results in the case of zero noise

The equation of motion in the presence of brownian noise using langevin equations are given as

$$\begin{aligned}
\frac{x(t)}{R} =& e^{-\gamma D_r t}[c_x + f(D_r t, w, \theta_0, \gamma) \\
&+ \frac{1}{2}f(D_r t, w + \nu, \theta_0 + \phi, \gamma) \\
&+ \frac{1}{2}f(D_r t, w - \nu, \theta_0 - \phi, \gamma)]
\end{aligned} \tag{3.10}$$

and

$$\begin{aligned}
\frac{y(t)}{R} =& e^{-\gamma D_r t}[c_y + f(D_r t, w, \theta_0 - \frac{\pi}{2}, \gamma) \\
&+ \frac{1}{2}f(D_r t, w + \nu, \theta_0 + \phi - \frac{\pi}{2}, \gamma) \\
&+ \frac{1}{2}f(D_r t, w - \nu, \theta_0 - \phi - \frac{\pi}{2}, \gamma)]
\end{aligned} \tag{3.11}$$

If ratio of ν and w is rational, trajectories will be like closed rosette curves and if the ratio is irrational, path will never make closed curve. Here we have taken ratio rational in all condition for different w and ν which you an see in fig 3.3.
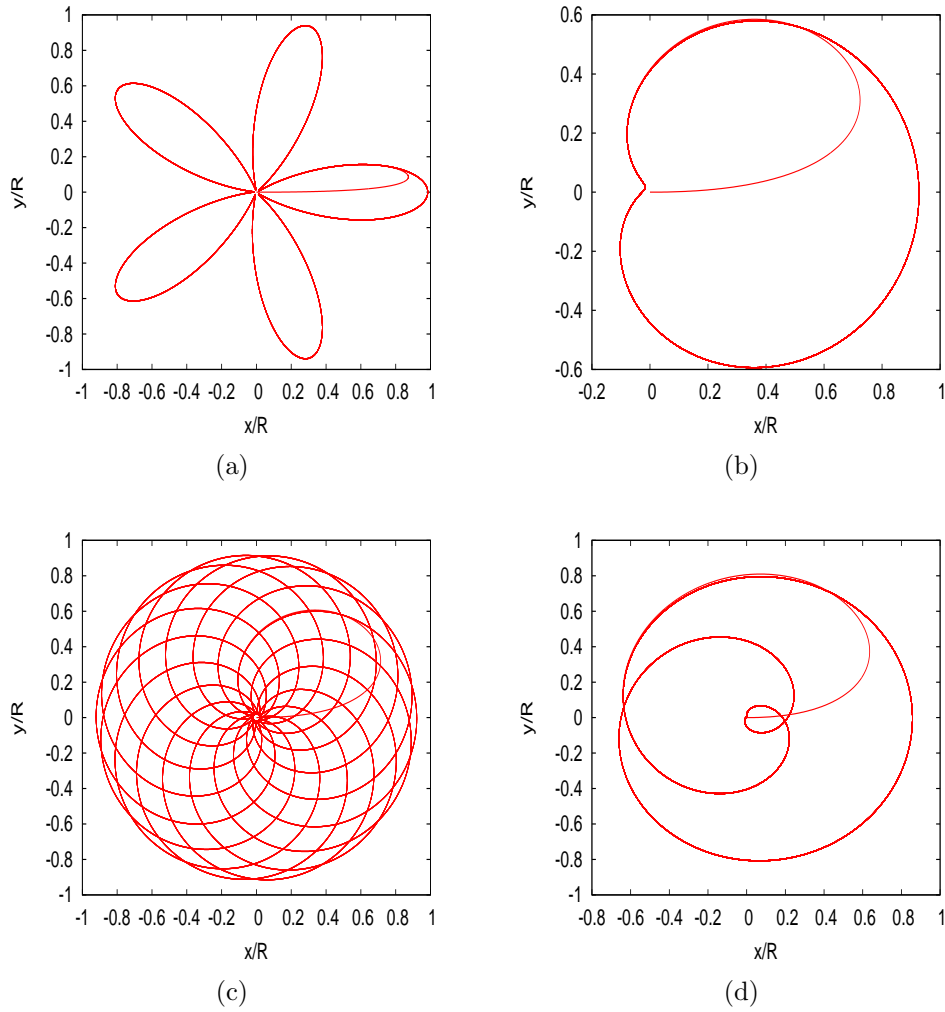
Figure 3.3: Noise free trajectories with constant $\gamma = 2$, $F_{p_0} = 1$ and $\theta_0 = \phi = 0$:(a)$\nu = 0.5$ and $w = 0.1$, (b)$\nu = 0.7$ and $w = 0.7$, (c)$\nu = 0.7$ and $w = 0.75$, (d)$\nu = 1.2$ and $w = 1.2$.

In the presence of brownian noise

By including brownian noise, the mean positions of circle swimmer in x-y direction are given as

$$
\begin{aligned}
\frac{\langle x(t) \rangle}{R} =& e^{-\gamma D_r t}[c_x + f(D_r t, w, \theta_0, \gamma - 1) \\
&+ \frac{1}{2} f(D_r t, w + \nu, \theta_0 + \phi, \gamma - 1) \\
&+ \frac{1}{2} f(D_r t, w - \nu, \theta_0 - \phi, \gamma - 1)]
\end{aligned}
\tag{3.12}
$$

17

and

$$\frac{\langle y(t) \rangle}{R} = e^{-\gamma D_r t}[c_y + f(D_r t, w, \theta_0 - \frac{\pi}{2}, \gamma - 1)$$
$$+ \frac{1}{2} f(D_r t, w + \nu, \theta_0 + \phi - \frac{\pi}{2}, \gamma - 1) \qquad (3.13)$$
$$+ \frac{1}{2} f(D_r t, w - \nu, \theta_0 - \phi - \frac{\pi}{2}, \gamma - 1)]$$

So we can see in the fig 3.4 that number of petals is same as earlier in the case of free noise trajectories but due to rotaional noise, subsequent petals goes smaller inside the earlier petals in next period.
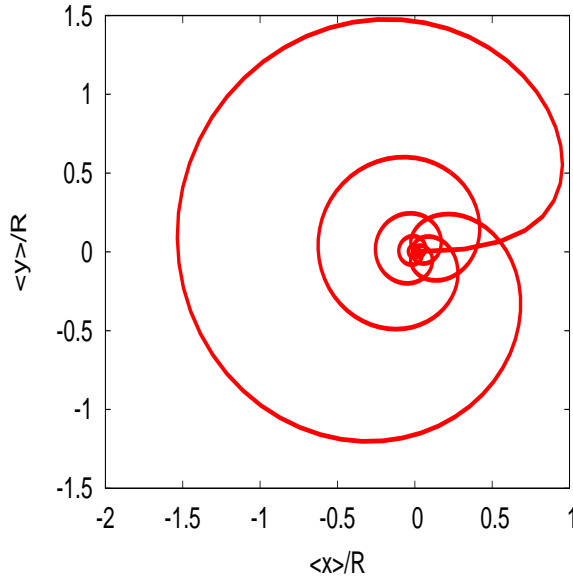

Figure 3.4: Nose averaged trajectories with constant $\gamma = 50$, $F_{p_0} = 50$, $\theta_0 = 0$, $\phi = 3\frac{\pi}{2}$, $\nu = 7$ and $w = 14$.

3.3   Time-Dependent Harmonic Potential

Now we study the dynamics of a circle swimmer in time varying harmonic trap potential and keep the self-propulsion force value fixed and the equation of harmonic potential is given as

$$\gamma(t) = \gamma_0[1 + cos(\Omega t)] \qquad (3.14)$$

where Ω is breathing frequency. This means that the swimmer is under the influence of a trap which is opening and closing.

In the absence of brownian noise

Now we have studied the motion of a circle swimmer in time dependent harmonic trap similiar to earlier case with time dependent self propulsion. Here the trajectories are determined by circle swimming and time dependent of the trap potential. So most of the trajectories have many petals fig 3.5. In fig. 3.5(a), you can see that there are three petals because breathing frequency $\Omega = 1.5$ is three times larger than circling frequency $w = 0.5$ and we have also shown here many trajectories with different Ω and w fig. 3.5.
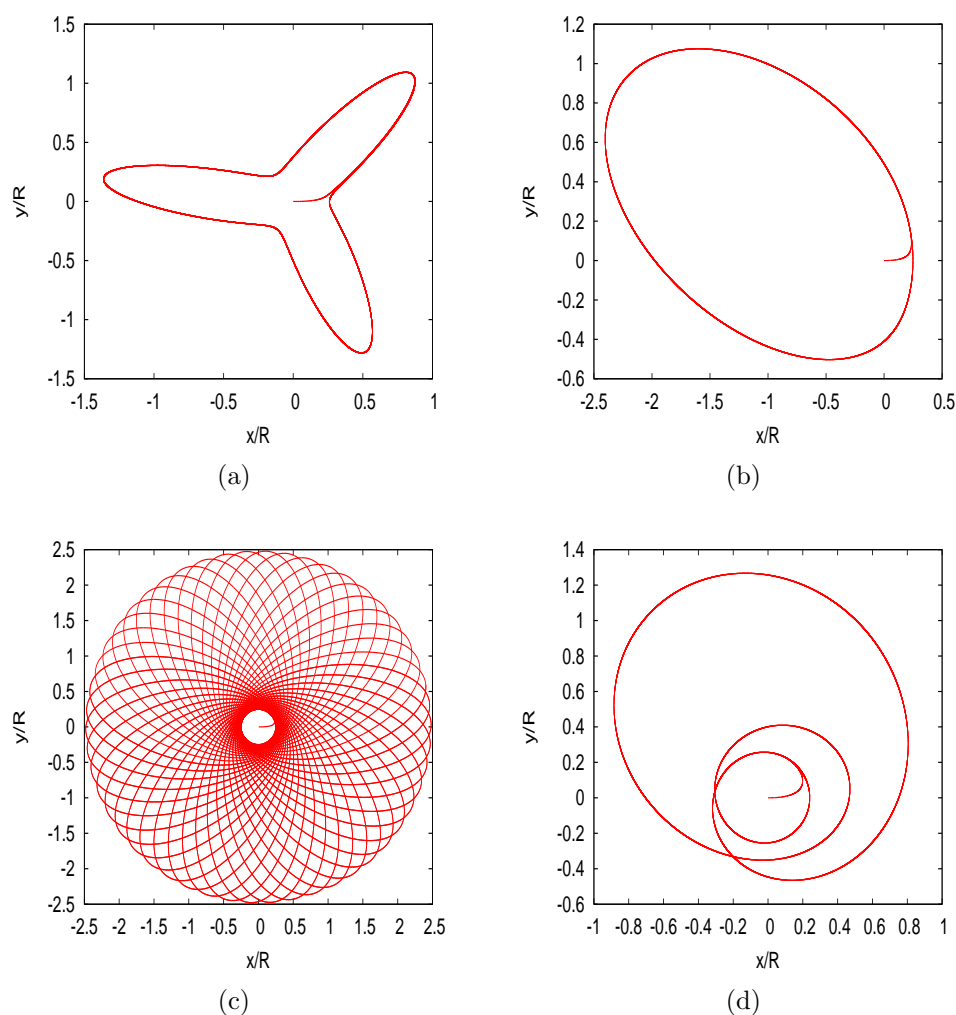

Figure 3.5: Nose free trajectories with constant $F_p = 1$, $\theta_0 = 0$ and $\gamma_0 = 2$. (a)$\Omega = 1.5$ and $w = 0.5$, (b)$\Omega = 0.5$ and $w = 0.5$, (c)$\Omega = 0.5$ and $w = 0.51$, (d)$\Omega = 0.4$ and $w = 1.2$.

Conclusion:

In the absence of noise, the circle swimmer in the presence of the harmonic trap shows periodic trajectories. The period of the trajectories is determined by the frequencies of the swimmer and those due to the time dependent trap or time dependent self propulsion. In the presence of noise, the trajectories are spiral curves collapsing towards trap center.

Chapter 4

Active Particles in Two-Dimensional Trap

Having studied the dynamics of a single circle swimmer in a harmonic trap, under different trap condition, we now looks at the collective dynamics of a large number of interacting active particles in a harmonic trap. Many body systems under different type of confinement is relevant in several situation. Here, we study active particles which unlike the circle swimmer only has rotational diffusion.

4.1 Model and Simulation

We consider active particles interacting via standard repulsive potential. We numerically integrate the langevin equations of N active particles in a harmonic trap $V(r) = \gamma r^2$ interacting via WCA potential where $r^2 = x^2 + y^2$.

As before, position(r_i) and self-propulsion direction(θ_i) of particles completely specify state of the system. Time evolution of particles is obtained by the overdamped Langevin equations,

$$\dot{r}_i = D\beta[F_{ex}(r_i) + F_h(r_i) + F_p\hat{\mathbf{v}}_i] + \sqrt{2D}\eta_i^T \tag{4.1}$$

$$\dot{\theta}_i = \sqrt{2D_r}\eta_i^R \tag{4.2}$$

where,$F_h(r) = -\frac{dV(r)}{dr}$ and $F_{ex}(r) = -\frac{dU_{ex}(r)}{dr}$.
$U_{ex}(r)$ is called the WCA potential, given by,

$$U_{ex}(r) = \begin{cases} 4\epsilon\left[\left(\frac{\sigma}{r}\right)^{12} - \left(\frac{\sigma}{r}\right)^6 \right] + \epsilon & \text{if } r < 2^{\frac{1}{6}} \\ 0 & \text{otherwise} \end{cases} \tag{4.3}$$

σ is particle diameter, ϵ is the strength of interaction potential.

Local Structures of system

Here we have simulated the dynamics of active system in harmonic trap at different peclet number and you can see that at low peclet number active particles are packed tightly towards trap center beacause of lack of activation in system which you can see in fig. 4.1.
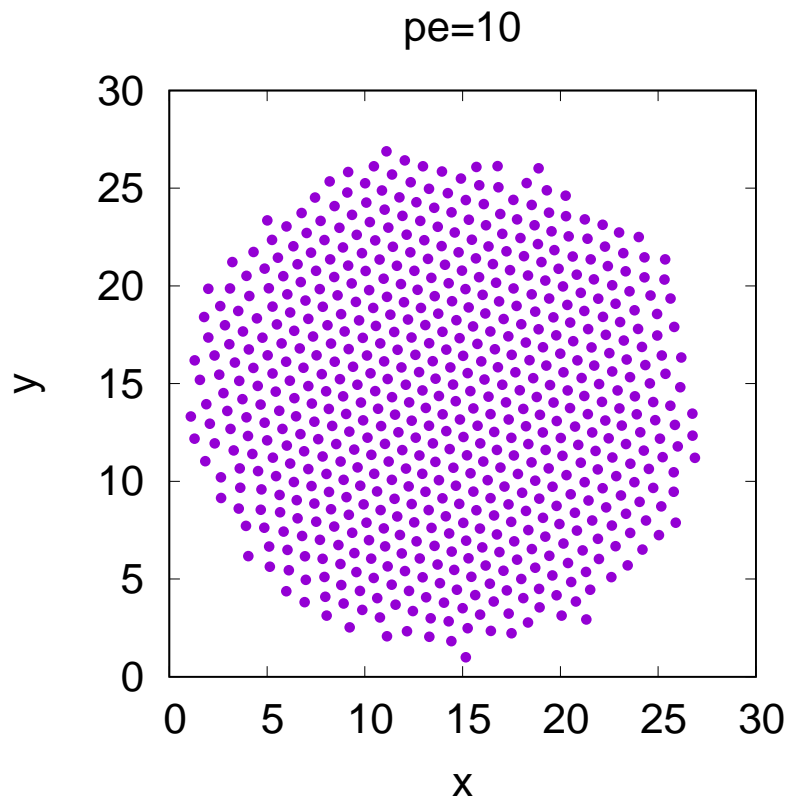

Figure 4.1: snapshot of the system configuration at Pe=10.

For higher peclet number, particle have higher activity and move out of trap and don't make compact structure which you can see in fig. 4.2. After that we have characterized these different local structures of active particles by radial distribution function in next part.
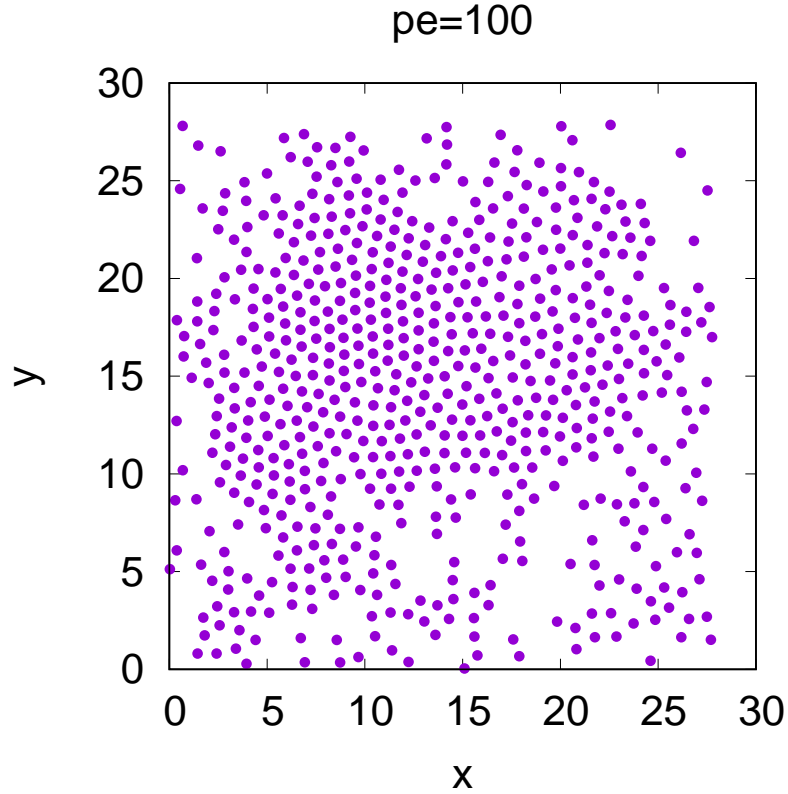
Figure 4.2: snapshot of the system configuration at Pe=100.

4.1.1 Radial Distribution

Here i have shown the radial distribution by gradually increasing the Peclet number (Pe) which you can see in fig 4.3. Within the cluster, the activity of the particles increases with Pe which lead to a broader cluster.

Fig 4.3 shows the stationary radial N-body density distribution for $N = 625$ particles for different values of the Pe number.

We can see that within the cluster, the particles have organized in concentric circles giving rise to undulations of the density with the typical period which is given by the minimal distance between particles. Other parameters are $D_r = 0.04$ and $\gamma = 2$. So with increasing Pe number, undulations in the radial distribution decreases.

On the other hand, the cluster expands and the local packing fraction decreases for large value of Pe basically at weak confinement .
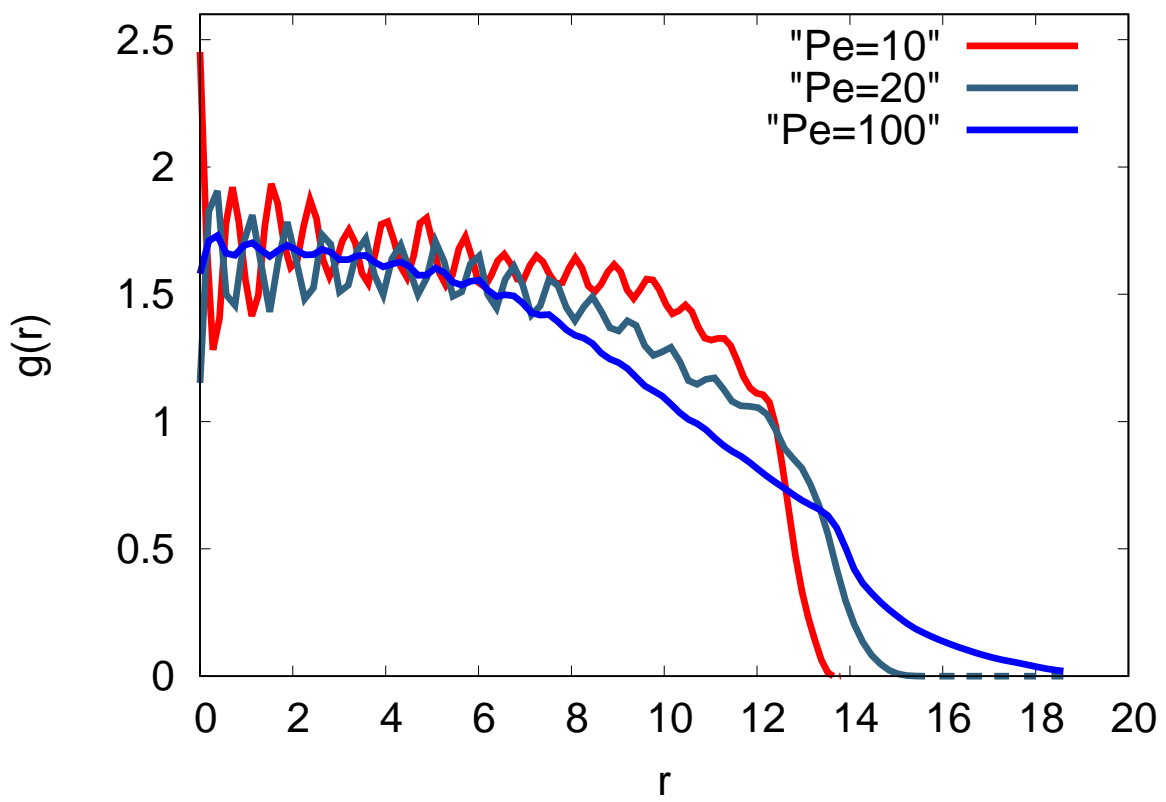
Figure 4.3: Comparision of pair distribution function with increasing Pe

Bibliography

[1] http://universe-review.ca/I15-86-fish.jpg

[2] http://www.pacificnorthwestbirds.com/wp-content/uploads/2013/08/starlings.jpg

[3] https://www.ph.ed.ac.uk/icmcs/research-themes/soft-matter-physics

[4] T. Vicsek and A. Zafeiris, Phys. Rep. 517, **71** (2012).

[5] Gabriel S Redner, Michael F Hagan, and Aparna Baskaran, Phys. Rev. Lett. **110**, 055701 (2013)

[6] Markus Rein, Thomas Speck, Eur. Phys. J. E 39, **84** (2016).

[7] A. Pototsky and H. Stark, EPL, **98** (2012) 50004

[8] Soudeh Jahanshahi, Hartmut Lowen, and Borge ten Hagen, PHYSICAL REVIEW E **95**, 022606 (2017)